Overview of Orion Crew Module and Launch Abort Vehicle Dynamic Stability

D. Bruce Owens* **and Vanessa V. Aubuchon†**
NASA Langley Research Center
Hampton, VA 23681

With the retirement of the Space Shuttle, NASA is designing a new spacecraft, called Orion, to fly astronauts to low earth orbit and beyond. Characterization of the dynamic stability of the Orion spacecraft is important for the design of the spacecraft and trajectory construction. Dynamic stability affects the stability and control of the Orion Crew Module during re-entry, especially below Mach = 2.0 and including flight under the drogues. The Launch Abort Vehicle is affected by dynamic stability as well, especially during the re-orientation and heatshield forward segments of the flight. The dynamic stability was assessed using the forced oscillation technique, free-to-oscillate, ballistic range, and sub-scale free-flight tests. All of the test techniques demonstrated that in heatshield-forward flight the Crew Module and Launch Abort Vehicle are dynamically unstable in a significant portion of their flight trajectory. This paper will provide a brief overview of the Orion dynamic aero program and a high-level summary of the dynamic stability characteristics of the Orion spacecraft.

Nomenclature

cg	=	center of gravity
C_A	=	axial force coefficient
C_N	=	normal force coefficient
C_m	=	pitching moment coefficient
Cm_q	=	damping-in-pitch coefficient, $\frac{\partial C_m}{\partial (q \cdot lRef/2V_\infty)} + \frac{\partial C_m}{\partial (\dot{\alpha} \cdot lRef/2V_\infty)}$, per radian
C_n	=	yawing moment coefficient
Cn_r	=	damping-in-yaw coefficient, $\frac{\partial C_n}{\partial (r \cdot lRef/2V_\infty)} + \frac{\partial C_n}{\partial (\dot{\beta} \cdot lRef/2V_\infty)}$, per radian
f	=	frequency, Hz
k	=	reduced frequency parameter, $\omega * lRef/V_\infty$
$lRef$	=	reference length, maximum diameter of the CM heatshield, ft.
M	=	Mach number
$\overline{q}_\infty$	=	freestream dynamic pressure, psf
$\hat{p}, \hat{q}, \hat{r}$	=	non-dimensional roll rate, $p*lRef/2V_\infty$; pitch rate, $q*lRef/2V_\infty$; yaw rate, $r*lRef/2V_\infty$; respectively
Re_d	=	Reynolds number, $V_\infty * lRef/\nu$
$sRef$	=	reference area, ft^2
V_∞	=	freestream velocity, ft/s
t	=	time, seconds

*Aerospace Engineer, Flight Dynamics Branch, NASA LaRC, AIAA Associate Fellow
†Aerospace Engineer, Flight Dynamics Branch, NASA LaRC, AIAA Senior Member

x/D, z/D = x and z locations of the cg non-dimensionalized with respect to the maximum CM heatshield diameter and measured relative to the CM afterbody cone theoretical apex.

α = angle of attack, deg.

β = angle of sideslip, deg.

ν = kinematic viscosity, ft^2/s

ω = oscillatory frequency ($2\pi f$), rad/s

ρ = density, $slug/ft^3$

ALAS = Alternate Launch Abort System

ARC = Ames Research Center

ARF = Aeroballistic Research Facility, Eglin Air Force Base

BR = Ballistic Range

CAP = CEV Aerosciences Project

CFD = Computational Fluid Dynamics

CM = Crew Module

CPAS = CEV Parachute Assembly System

EDL = Entry, Descent, and Landing

GDF = Gun Development Facility, NASA ARC

GN&C = Guidance, Navigation, and Control

HFFAF = Hypervelocity Free-Flight Aerodynamics Facility, NASA ARC

LAMP = Large Amplitude Multi-Purpose Facility

FO = Forced Oscillation

FTO = Free-to-Oscillate

LaRC = Langley Research Center

LAT = Launch Abort Tower

LAV = Launch Abort Vehicle

MRC = Moment Reference Center of the CM (theoretical apex of the after cone)

OML = Outer Mold Line

PA-1 = Pad Abort 1

TDT = Transonic Dynamics Tunnel, NASA LaRC

TRF = Transonic Range Facility, Aberdeen Proving Ground

VST = 20-Foot Vertical Spin Tunnel, NASA LaRC

I. Introduction

NASA, Lockheed Martin, and its subcontractors are designing and building a manned spacecraft for the purpose of sending humans to Low Earth Orbit (e.g., the International Space Station) and beyond. The Orion spacecraft consisting of Launch Abort Tower (LAT), Crew Module (CM), Service Module (SM), and Spacecraft Adapter (SA) is shown in Fig. 1. The CM alone and the Launch Abort Vehicle (LAV), which includes the Launch Abort Tower (LAT) plus the CM, are the two vehicles of Orion that will experience atmospheric flight where dynamic stability is a concern. Characterization of the dynamic stability of the CM and LAV is important because they are dynamically unstable in the trim region of heatshield-forward flight, which will occur in Earth atmospheric flight on re-entry or launch aborts. The dynamic instability of the CM will cause it to tumble in free-flight (i.e., closed-looped flight control system inactive). Without an active closed-looped flight control system, the dynamic stability characteristics of the LAV will cause either a coning motion or tumble from heatshield-forward free-flight. Figure 2 shows the concept of operations for a launch abort. At abort initiation the abort motor fires, causing the LAV to separate from the launch vehicle. There is a period of tower-forward flight, followed by a reorientation phase during which the LAV rotates into heatshield-forward flight. An active control system, via an attitude control motor at the top of the LAV, is used for stability and control. There is sufficient vehicle angular rate during the reorientation maneuver such that the dynamic aerodynamics produce a significant contribution to the overall aerodynamics. After reorientation, aerodynamic damping plays a significant role in the number of overshoots for abort regimes where dynamic pressure is high. For the CM there are periods of free-flight between LAT jettison and drogue inflation and between drogue release and main chute inflation, where its dynamic instability can significantly affect the trajectory of the CM. Also, with sufficient body angular rates at drogue inflation, the CM dynamic aerodynamics can contribute to unacceptable motions while flying under the drogues.

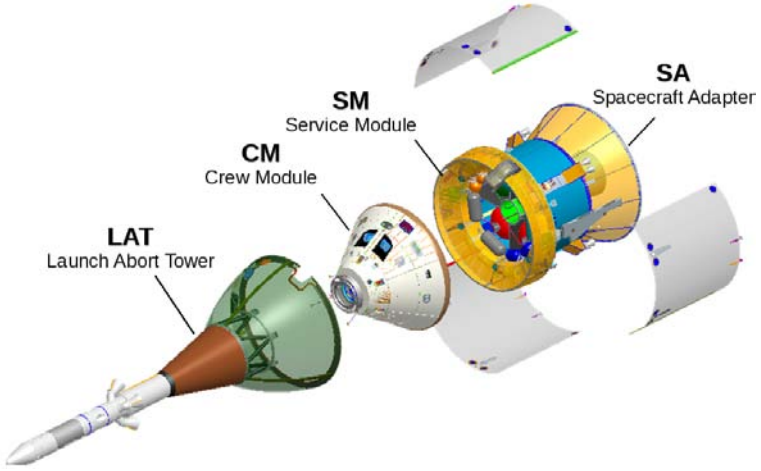

Figure 1. Illustration showing the various parts of the Orion spacecraft.

Figure 2. Illustration of the concept of operations for an abort from the launch vehicle.

The importance of accurately determining the dynamic aerodynamic instabilities of blunt-body vehicles has been evident since at least the Mercury program (Ref. 1). The Apollo program devoted considerable resources toward characterizing the dynamic stability of the Command Module and Launch Escape Vehicle (Ref. 2). Since the Orion CM is very similar to the Apollo Command Module, the dynamic aerodynamic tests from the Apollo project provided valuable insight into damping characteristics of the Orion CM. Some of the differences between them are the OML, moments of inertias, and cg location. Because any of these differences can affect dynamic stability, new tests were required. Also, advancements in test techniques since the Apollo program make possible a refined characterization of the dynamic stability.

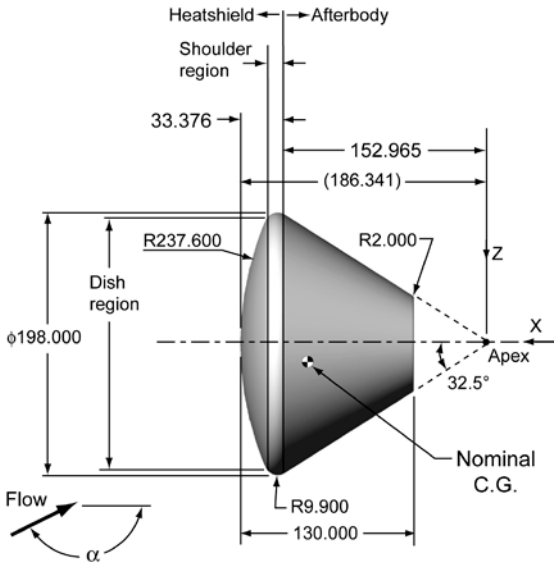

Figure 3. Sketch of the Orion Crew Module reference OML used in dynamic aero testing.

Although other configurations were tested in the Orion dynamic aero program, there were three main OMLs that were used in the vast majority of the tests. Figure 3 shows a sketch of the smooth reference OML used for the Crew Module dynamic stability tests. Two different launch abort vehicle configurations were tested. One is the current production spacecraft called

Alternate Launch Abort System (ALAS) (see Fig. 4). The other configuration tested is designated -068 and was used for the first flight test vehicle called Pad Abort -1 (PA-1) (see Fig. 5). The OML for PA-1 is different than the production version (ALAS) as the lines for the production version continued to evolve after the lines for the PA-1 vehicle were frozen in order to meet the flight test launch date.

The coordinate system used in the dynamic stability tests is shown in Fig. 6. In the text nose-forward flight is equivalent to $\alpha = 0°$ and heatshield-forward flight is equivalent to $\alpha = 180°$. The MRC shown in this figure is the one used for static data. All aerodynamic data derived from dynamic stability tests are at the flight cg that was current as of model fabrication.

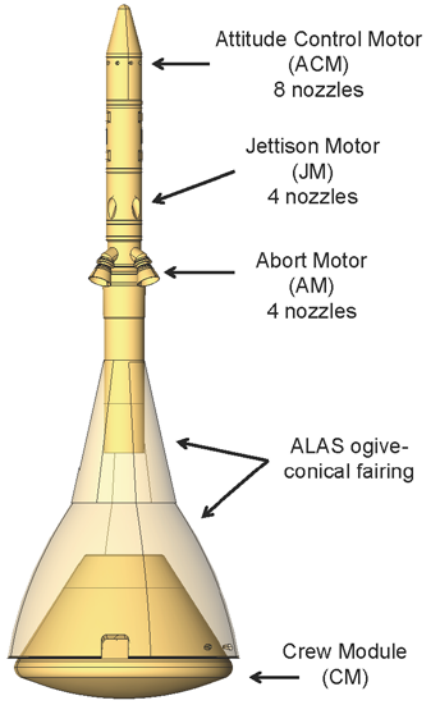

Figure 4. Illustration of the Orion ALAS Launch Abort Vehicle OML used in dynamic aero testing.

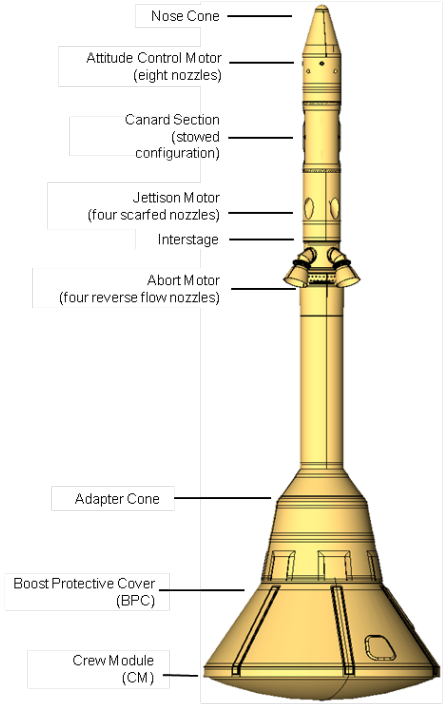

Figure 5. Illustration of the Orion PA-1 Launch Abort Vehicle OML (-068) used in dynamic aero testing.

At the beginning of the Orion wind tunnel test program the dynamic aero tests were exploratory. Confidence in the ability to accurately characterize the dynamic aero would require corroborating test results from various test techniques. Therefore, both captive wind tunnel tests, including forced and free oscillation techniques, and free-flight tests in ballistic ranges were conducted. This paper will give an overview of the test techniques, facilities, models, and test results employed by the Orion Aerosciences group, called CEV Aerosciences Project (CAP), to characterize the dynamic stability of the Orion spacecraft. The paper will begin with a brief discussion of the similitude requisites. Next, the various test techniques and the facilities in which they are used will be described, followed by a description of the models used, along with how similitude laws and facility size dictate model sizing, instrumentation, and structural requirements. Then, an overview of the CM and LAV dynamic stability will be given in terms of the "damping derivatives". For the purposes of this overview, the use of the phrase damping derivative means either Cm_q or Cn_r, as defined in the nomenclature, because the CM and LAV are essentially axis-symmetric vehicles. A summary of the Orion dynamic aero program will conclude the paper.

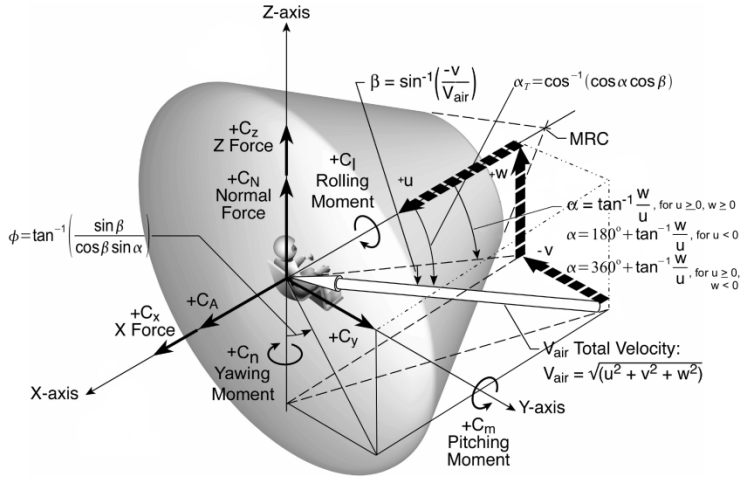

Figure 6. Coordinate system used in the dynamic stability tests of the Orion spacecraft models.

II. Similitude Requirements

Similitude requirements for dynamic testing are given in numerous documents with Refs. 3 and 4 being good examples. In general, dynamic scaling guarantees that the induced flow field produced in ground tests is the same as that which occurs in full-scale flight. The first dynamic scaling consideration is whether to incorporate Froude or Mach scaling. Froude scaling guarantees that the model's attitude will be accurately predicted while Mach scaling is used to properly account for compressibility effects in the dynamic model. It is a challenge in model building and test technique apparatus performance to match Froude *or* Mach requisites, let alone match them both. In practice, they are matched to the extent possible as governed by test technique, model building capabilities, cost, time, and desired data accuracy. The specific similitude requirements for each technique will be addressed in the subsequent sections.

III. Test Techniques

Both captive and free-flight dynamic test techniques were used in the characterization of the dynamic stability of the Orion spacecraft. Those tests techniques are single-degree-of-freedom (1-DOF) forced oscillation (FO), 1-DOF free-to-oscillate (FTO), ballistic range (BR) free-flight, and vertical wind tunnel free-flight. A summary of the various techniques used in the Orion project have been discussed in Ref. 5. The details of the test techniques given here will provide an update or additional information. The captive test techniques allow direct measurement of the forces and moments during dynamic motion of the model at the cost of limiting that motion to 1-DOF motion. Since the Orion spacecraft are essentially axis-symmetric the error from using a 1-DOF system is minimized. Even so, the Orion project chose to use 6-DOF free-flight tests either in a vertical wind tunnel and/or ballistic range to validate the dynamic aero model derived from 1-DOF methods. The free-flight methods allow the best representation of the full 6-DOF motion at the cost of having to derive the damping from the vehicle states using parameter identification methods such as those described in Ref 6. Table 1 summarizes the dynamic stability tests conducted for the Orion dynamic aero program. The captive techniques will be discussed first, followed by the free-flight techniques.

Table 1. Dynamic Stability Tests Conducted in Support of the CAP Aerodynamic Program

CAP ID	Model	Facility	Approx. Test Dates	Test Type	Purpose
8-CD	8.6% CM	TDT	Apr 06	Forced Oscillation	exploratory
11-CD	2.2% Apollo-like CM	TRF	Apr 06	Free-flying BR	exploratory
13-CD	1.3% CM	EBR	Mar 06	Free-flying BR	exploratory
14-CD	0.71% CM	HFFAF	Aug 06 / Mar 07	Free-flying BR	validation
15-CD	2.19% CM	TRF	Summer 06	Free-flying BR	exploratory
18-CD	8.6% CM	TDT	Apr 07	Forced Oscillation	database development
27-AD	11% PA-1 LAV, 11% ALAS, & 8.6% CM	TDT	Feb 08	Static F&M, Forced Oscillation, & Free-to-oscillate	database development
29-CD	0.4% CM	GDF	Aug 07	Free-flying BR	validation
45-AD	3.45% PA-1 LAV	VST	Jan 07	Free-flying Tunnel	early quick look assessment
46-AD	1.2% ALAS LAV	EBR	Apr 08 / Jan 09 / Jun 10	Free-flying BR	validation
48-CD	6.25% CM	VST	Apr 07	Free-flying Tunnel	validation
82-CD	6.25% CM	VST	Dec 07	Static F&M, Forced Oscillation	aero model development
108-CD	6.25% IDAT CM	LAMP	Aug 09	Forced Oscillation	IDAT OML assessment
109-CD	6.25% CM	VST	Dec 09	Free-flying Tunnel	IDAT drogue config. assessment
117-CD	6.25% CM	VST	Aug 10	Static F&M, Forced Oscillation	drogue damping assessment

A. Forced Oscillation

The forced oscillation (FO) technique is a captive 1-DOF method that uses an internally-mounted strain gauge balance along with angular rate measurements to compute the damping derivatives. Although arbitrary motion can be imparted, typically the models are forced to oscillate in a sinusoidal motion, as this is the most common motion observed when aircraft and spacecraft are free to oscillate. All of the Orion forced oscillation tests used sinusoidal motion at various frequencies and amplitudes. The additional similitude requirements beyond those for static testing include matching non-dimensional angular rate and reduced frequency parameter, *k*. The FO technique provides a measurement of the damping derivatives over a large angle-of-attack range without the use of special models. Unlike the FTO and BR technique, the model mass properties do not have to be scaled for FO. As the spacecraft design matures the mass properties and flight trajectories can change, resulting in a different frequency and rate of oscillation. The FO technique used in the Orion project measured the damping derivatives over a large range of frequencies and rates that cover the expected design space.

The first FO entry (8-CD) into the Transonic Dynamics Tunnel (TDT) was an exploratory test. The test used the portable LaRC Dynamic Stability Research System which includes a set of balances and special data acquisition hardware. A detailed explanation of this forced oscillation system including data acquisition requirements are given

in Ref. 7. This method uses a special internally mounted strain gauge balance designed to measure the dynamic stability derivatives as an equivalent mass-spring-damper second-order system and has been used for decades and was employed by the Apollo program. This model mounts in the traditional aft sting arrangement. At the time of the Apollo program the tests were conducted in the NASA Langley 8-FT Transonic Pressure Tunnel. The size of the test section limited the model size making it too small to be oscillated at the proper rotation point, which is the vehicle center of gravity. The data from these tests were deemed unacceptable and, therefore, not used in the final aero database for Apollo. Therefore, the Orion tests were conducted in the TDT in part because the 16-ft square cross-section allowed for a model large enough to mount the rotation point at the desired flight-derived cg location. Another reason that the TDT was chosen is that the model can be tested in an R134a gas medium. The properties of R134a gas assist in fulfilling the similitude requisites. The R134a has a density approximately four times higher and speed of sound half that of air. The increased density greatly increases Reynolds number, and the speed of sound reduction helps match non-dimensional rates and reduced frequency scaling parameters by reducing free-stream velocity for a given Mach number.

Since this test was exploratory, a large number of parameters were varied: model OML – apex cone closure (Apollo tested this way) and truncated apex, Mach number, angle-of-attack, oscillation frequency, Reynolds number, sting entry angle for sting interference, and cg for comparison to ballistic range data. The model size (8.63% or *lRef* = 17 inches) was chosen so the special oscillating balance could be placed in the model at the correct rotation point, for aerodynamic and inertia loading requirements, and for the desire to obtain a high Reynolds number. In this test, Mach number was varied from 0.3 to 1.1 with the majority of the testing in the transonic regime. Reynolds number based on *lRef* was varied from 1 to 10 million. Angle of attack was varied from 150° to 196° and oscillation frequency varied from 4 to 7 Hz at an amplitude of 1 degree. In addition to measuring the damping derivatives, limited static and dynamic surface pressures on the aft body were recorded. A general, and sobering, conclusion was that all parameters varied impacted dynamic stability. The effect of a sting on the damping derivatives was of special concern. This was addressed by having two different entry angles into the aft body. It was hypothesized that aft mounted stings disturb the wake flow, causing a change in the dynamic aero. Comparing the data (Fig. 7) from the two entry angles confirmed that sting placement does affect the damping derivatives significantly. This sting effect, and the desire to obtain higher non-dimensional rates and associated large amplitude effect, resulted in a follow-on test with a different approach being planned.

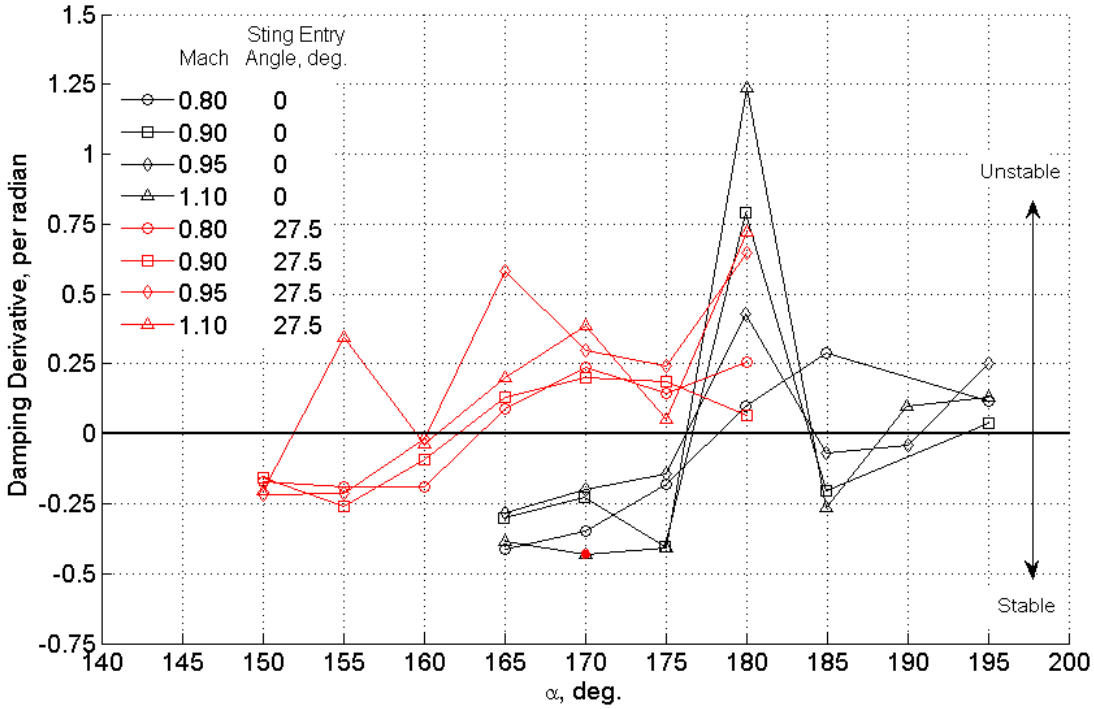

Figure 7. Sting interference on the damping derivative for two different aft sting entries in Test 8-CD for *M* = 0.8 to 1.1.

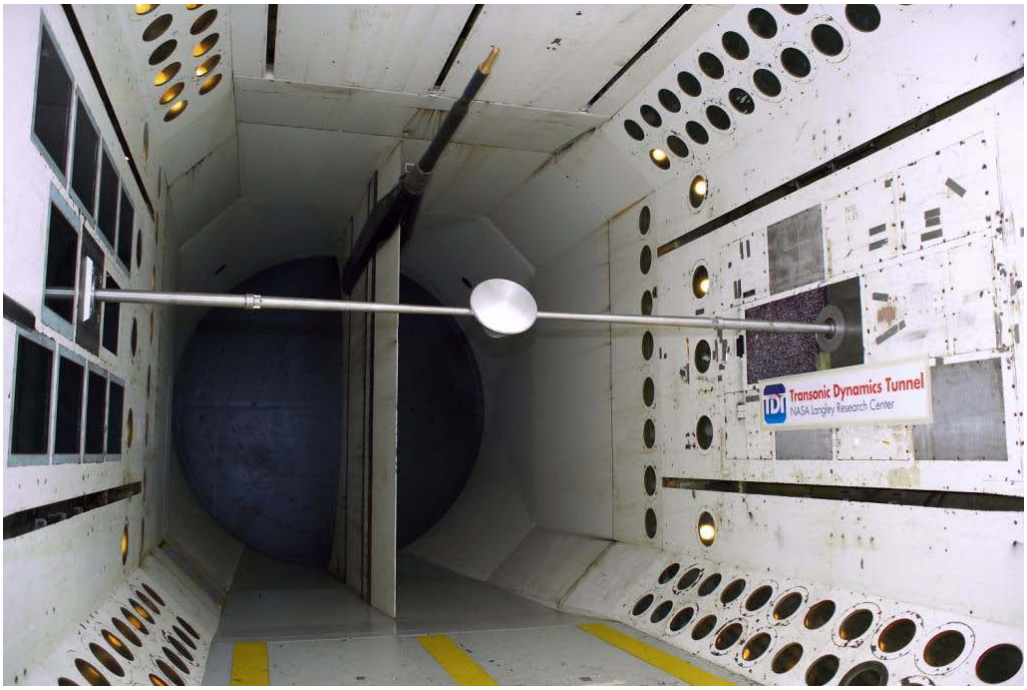

Figure 8. Orion 8.63%-scale Crew Module mounted to the traverse sting for forced oscillation and free-to-oscillate testing in the NASA LaRC Transonic Dynamics Tunnel.

In part to address issues found in Test 8-CD, the next two entries (18-CD and 27-AD) into the TDT used a newly designed forced oscillation system. This new apparatus was designed to mate to an existing hydraulically driven

oscillation system through a clutch and brake mechanism. This apparatus mounts the model to a sting that traverses the tunnel cross-section (see Figs 8 and 9).

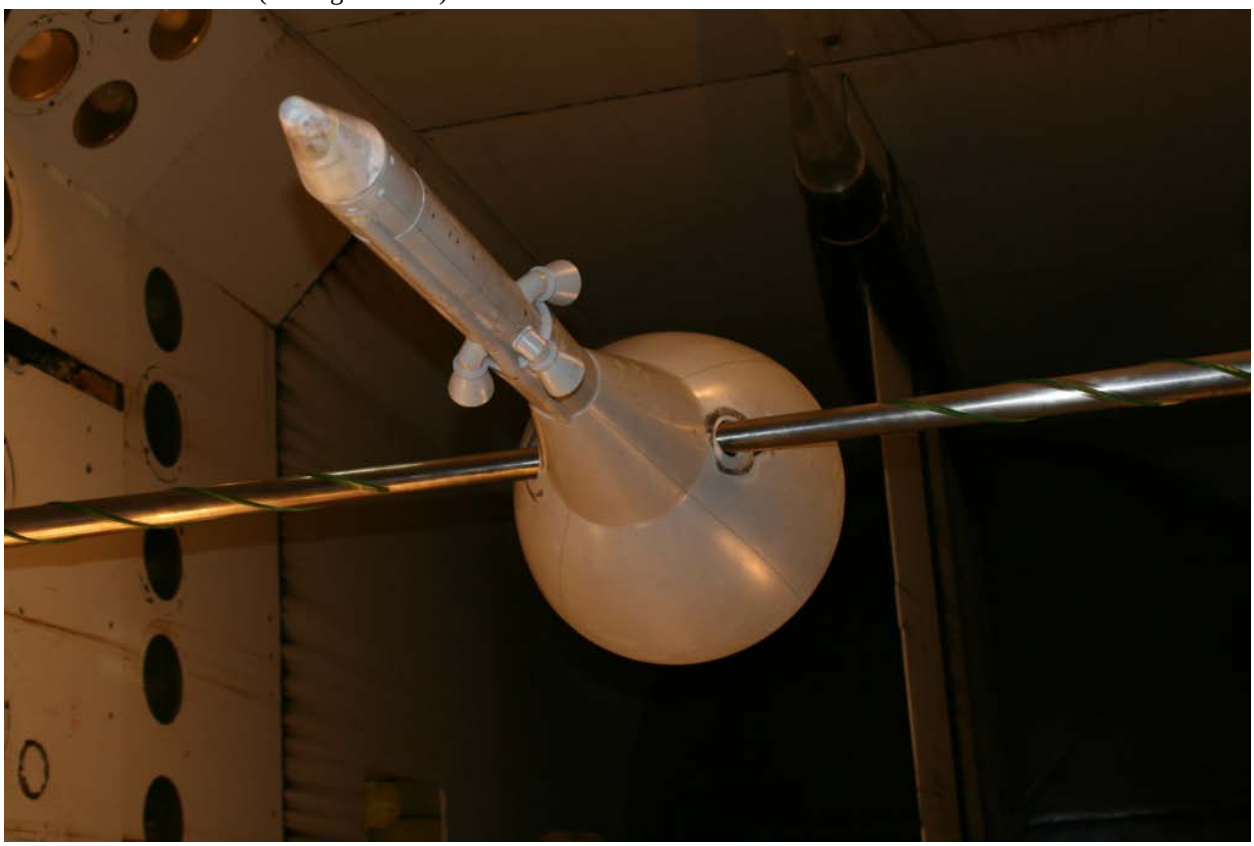

Figure 9. Orion 11%-scale ALAS Launch Abort Vehicle mounted to the traverse sting for forced oscillation and free-to-oscillate testing in the NASA LaRC Transonic Dynamics Tunnel.

The sting mates to the model at a location from the sides so that the model can be oscillated about the flight-derived cg. With the clutch-brake system the model could be tested in three modes – static force and moment, forced oscillation, and free-to-oscillate - without needing a separate tunnel entry or time to switch between modes. The new rig allowed for measuring data over the full 360° angle of attack range without a need for personnel to enter the tunnel. The hydraulic oscillation system is fully programmable, allowing for any motion within the torque limits of the drive system. Although any arbitrary motion was possible, only sinusoidal motion was imparted to the model at frequencies up to 9 Hz and amplitudes up to 40°. The limiting factor of 9 Hz was due to the first bending mode of the sting-model system being at 11Hz. The model was tested at Mach numbers from 0.2 to 1.1 with reduced frequencies and non-dimensional rates that were derived from Apollo flights, Orion spacecraft simulation studies, and the free-to-oscillate tests of the dynamically scaled model. The damping derivatives are computed using an internally-mounted six-component strain gauge balance and angular rates measured with a rate gyro or angle displacement transducer. This method is in contrast with the measurement system used in Test 8-CD, which used a special oscillating balance. More information on the data reduction method of Test 18-CD and 27-AD can be found in Ref. 8. The forced oscillation tests 18-CD and 27-AD are the main direct data sources for construction of the dynamic aero model for the Orion spacecraft aerodynamic database.

Within the CEV Aerosciences community there was considerable discussion involving the sting effect on the results of the 1-DOF methods. As previously stated, it is hypothesized that the aft-mounted sting disturbs the wake flow whereas the side-mounted sting influences the developing flow-field on the aft-body. Although the traverse-mounted sting does not eliminate sting effects, the sting effects are, at least, more constant with angle of attack compared to the aft-mounted sting. Also as a follow-up to the sting effects runs in Test 8-CD, there was an attempt

during the 18-CD entry to measure additional aft-sting effects. In this case a sting was brought into proximity of the model in the location an aft-mounted sting would be and then data were taken while oscillating the model with the transverse sting. Unfortunately, time constraints did not allow the opportunity to acquire adequate data to draw a conclusion. This lack of a conclusion points to an additional need for the free-flight tests.

Two low-speed forced oscillation tests, 82-CD and 117-CD, were conducted in the NASA LaRC 20-Foot Vertical Spin Tunnel (VST) to support the TDT tests and to provide a database for modeling the free-flight of the CM alone (VST Test 48-CD) and CM with drogues (VST Test 109-CD). The main objective of Test 82-CD was to assess potential modeling deficiencies, especially Cn_r. The test utilized the 1/16th-scale model (12.375 inch diameter heatshield) originally designed for the free-flying 48-CD test discussed subsequently. Test conditions were M = 0.04, V_∞ = 50 ft/sec, $\overline{q}_\infty$ = 3 psf, $\mathrm{Re_d}$ = 310,000. Model attitudes were α = 90° to 180° and β = -4° to 45°. The model was sting mounted through the side as in TDT so the rotation axis is about the correct cg location, with the difference being that it only mounts through one side (Fig. 10). The model was sinusodially oscillated at amplitudes up to 40° and frequencies up to 2 Hz. The range of reduced frequencies and non-dimensional rates encompassed the ones measured in VST free-flight tests 48-CD and 109-CD. The forced oscillation technique and data reduction utilized in the VST tests were the same as in the TDT tests. The test 117-CD objectives were to ascertain if the drogues had any impact on the CM dynamic

Figure 10 Test setup for FO Test 82-CD in the VST.

Figure 11. Test setup for FO Test 117-CD in the VST

stability and to measure the total system damping provided by the combination of the CM and drogue(s) (Fig. 11). In addition, a load cell measured the drogue(s) riser line force. The results of Test 117-CD are given in Ref. 9.

During the summer of 2009 the Integrated Design Analysis Team (IDAT) was organized to address a number of design considerations of the CM, with one area being entry-descent-landing (EDL). The outcome of these design trade studies was the need for more volume in the forward bay area. Given the theory that when flying heatshield-forward aft-body shape affects the dynamic stability and the inability of CFD to quickly ascertain this effect, a quick assessment wind tunnel test was conceived. At the time of the IDAT studies the NASA LaRC VST was unavailable. Instead, and so that the existing 82-CD model could be employed, the Bihrle Applied Research Large Amplitude Multi-Purpose (LAMP) facility was chosen because it was immediately available and with similar model mounting hardware as the VST. The LAMP facility is a low-speed vertical wind tunnel with a circular test section of 10 ft. diameter. It is mainly used for obtaining the oscillatory and rotary derivatives of spinning aircraft. The test (108-CD) was a low-speed forced oscillation test to assess the IDAT OML potential changes to the CM dynamic stability. The various IDAT OMLs were achieved by retrofitting the 82-CD 1/16th-scale model with components constructed from rapid prototyping techniques. A total of ten different configurations were evaluated. Since this facility would

provide similar low-speed, low Reynolds number test conditions as the VST, the results of this test were compared to 82-CD for assessing any dynamic stability changes caused by the different configurations. The results showed that none of the IDAT candidate OMLs significantly altered the dynamic stability. This test was conceived, conducted, and results presented to the design team within a month. The test is a good example of how this technique, coupled with rapid-prototyping model fabrication, can provide timely answers during the conceptual design phase.

B. Free-to-Oscillate

Free-to-Oscillate (FTO) tests were conducted in the TDT and VST tunnels. A brief exploratory style FTO test was conducted in the VST to assist in the data analysis of the VST free-flying test 48-CD. This FTO apparatus constrains the model to only rotate about a single axis, in this case pitch, but the model is free to translate about three-axes in the tunnel. As previously mentioned, FTO tests were conducted during test 27-AD in the TDT. In general, the FTO technique is used in the suite of test techniques to obtain a more comprehensive characterization of the dynamic stability of the model. In 27-AD, the rig was designed specifically so that static force and moment, forced oscillation, and free-to-oscillate methods could all be done with the same model using the same support system with no time required to change between test techniques. In order to conduct FTO tests additional considerations are necessary beyond static force and moment and forced oscillation. These considerations are the following: ballasting the model cg to be on the axis of rotation, dynamic scaling of the moment of inertia about the axis of rotation, and having very low friction in the rotating support system. The friction must be measured if aerodynamic damping is going to be extracted from the FTO time history data, since the friction acts as artificial damping that must be distinguished from the aerodynamic damping.

FTO testing provides a number of benefits. One benefit is that the FTO runs were another data source for determining the reduced frequency parameter values to use during the FO runs. During test 27-AD the FTO runs were conducted first, followed by forced oscillation using the reduced frequency parameter determined from the FTO runs. Since the static force and moment and forced oscillation data are time averaged results, another benefit is that the FTO attitude time history shows the integrated effect of the unsteady static and dynamic aero. Additionally, the FTO runs provide time history data from which aero extraction techniques can be used to determine aerodynamic damping. The Apollo program developed FTO aero extraction techniques that accurately predicted the values of damping as a function of angle-of-attack (Ref. 10). Example Orion CM and LAV FTO data sets will be shown in sections IV and V.

C. Ballistic Range

There were six ballistic range (BR) tests conducted to support characterization of the CM and LAV dynamic aero. The Apollo program and Mars entry vehicle programs also used the BR test technique. The BR tests conducted provide 6-DOF motion of the model from subsonic through high supersonic Mach numbers. These tests can be used in conjunction with wind tunnel test data to validate the Orion CAP dynamic aero model. As shown in Table 1, the model scale is typically very small with corresponding low Reynolds numbers. In BR tests, the models are fabricated so that the model has at least the same the longitudinal cg as the full-scale spacecraft but the weight and moments of inertias are not dynamically-scaled. Instead the weight and inertias are set to minimize deceleration down the range and decrease the frequency of oscillation in an attempt to get the most data points per oscillation cycle. Some BR facilities allow for lifting trajectories so an offset cg can be flown.

Test 11-CD and 15-CD were conducted at the Army Research Laboratory, Aberdeen Proving Ground Transonic Range Facility (TRF) in order to explore the advantages of an outdoor ballistic range using a highly instrumented 2.2%-scale CM. Some of the advantages of this test technique over indoor ballistic range techniques are a lifting trajectory with larger models, therefore higher Reynolds number, and a highly instrumented model that allows for a full description of the 6-DOF motion compared to only acquiring pitch and yaw attitudes. An indoor BR test has only a few discrete set of measurements of the trajectory whereas the outdoor BR trajectory is described with nearly a continuous set of data. Unfortunately, the sensor suite used in these tests did not provide adequate data fidelity to

obtain useful information on the dynamic stability of the CM. Even so, with further developmental tests this technique shows great promise in providing high quality free-flight data at high Mach numbers.

Test 13-CD (Ref. 11) was conducted in the Eglin Air Force Base Aeroballistic Research Facility (ARF) (Fig. 12) using a 1.3%-scale CM in order to characterize the dynamic stability at transonic Mach numbers. The test data showed that for transonic Mach numbers the trends in damping data near $\alpha = 180°$ match those of forced oscillation test 8-CD.

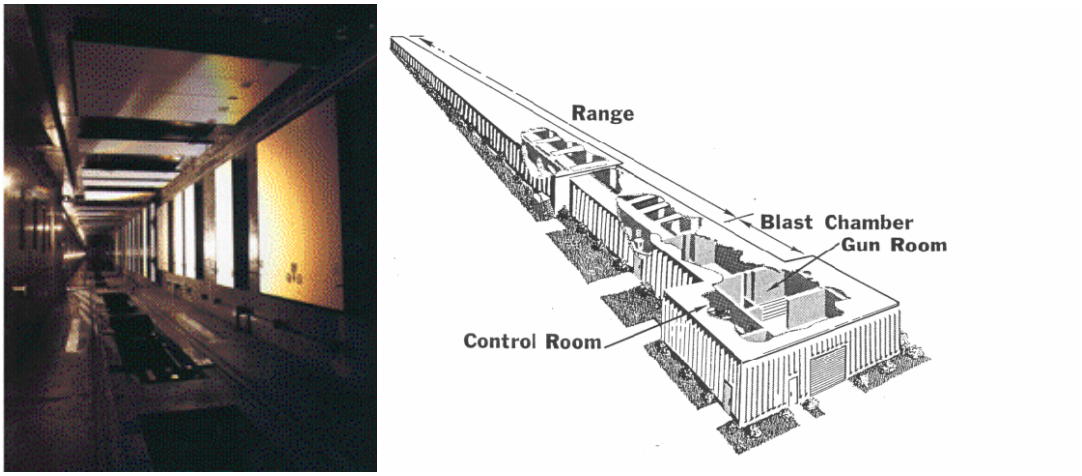

Figure 12. Eglin Aeroballistic Research Facility (ARF)

Figure 13. NASA-ARC Hypervelocity Free-Flight Aerodynamics Facility (HFFAF) test section

Test 14-CD was conducted in the NASA-ARC Hypervelocity Free-Flight Aerodynamics Facility (HFFAF) (Fig. 13) using a 0.71%-scale CM model. This BR test flew non-lifting and lifting models so that comparisons could be made to the BR test 13-CD and to the forced oscillation wind tunnel tests, 8-CD and 18-CD. Figure 14 shows a shadowgraph from the test. The test obtained damping in pitch and yaw data at M = 0.7, 1.1, and 1.25. At M = 0.7

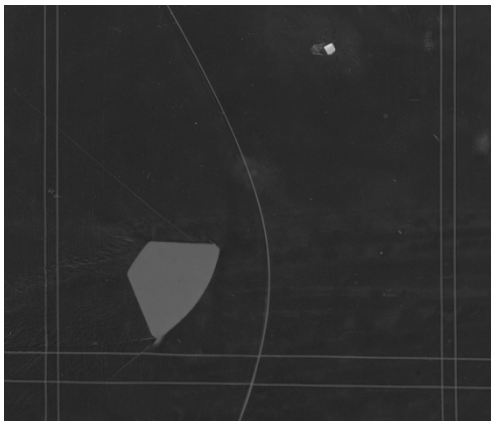

Figure 14. Shadowgraph of the CM model in the NASA-ARC Hypervelocity Free-Flight Aerodynamics Facility.

the results showed unstable damping at trim angles of attack similar to the 8-CD FO test but the α range and magnitude of unstable damping were markedly different. Also, the test results concluded that both lifting and non-lifting models exhibited dynamic stability for the α-range away from trim but that the lifting cases were more stable. A complete report on the details of this test is given in Ref. 12. This reference points out that while there is some agreement with the forced oscillation results there are some stark discrepancies that need further research.

Test 29-CD was conducted in the NASA-ARC Gun Development Facility (GDF) using a 0.4%-scale lifting CM model. Whereas the other BR tests were designed to get high Mach number damping derivatives, the trajectories for this BR test were designed to get subsonic damping data specifically at M = 0.3 and M = 0.7. The test results concluded that the CM model was dynamically unstable near α-trim for M = 0.3 but was inconclusive for M = 0.7.

Test 46-AD was conducted at the Eglin ARF and was the only LAV ballistic range test. The objective of the test was to obtain free-flight data on the ALAS LAV geometry to assist in the validation of the other dynamic stability tests. Flights initiating from tower-forward and heatshield-forward flight (shown in Fig. 15) were flown. Only heatshield forward flights were successfully achieved because the tower would break off when shot in the tower-forward orientation. The flights were designed to measure flight data for Mach numbers 0.7 to 1.6. Flights were made at two different x_{cg} locations. The flights provided enough data to derive damping values at M = 1.1 and M = 0.7 with higher accuracy for the M = 1.1 point. As shown with the other test techniques the LAV is unstable for angles of attack near 180°.

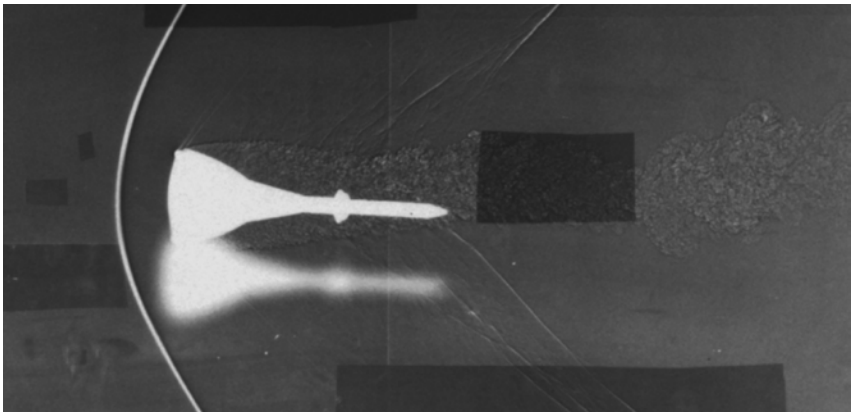

Figure 15. Shadowgraph of the LAV model in the Eglin ARF ballistic range.

D. Vertical Spin Tunnel Free-Flight

Three free-flight tests (45-AD, 48-CD, 109-CD) were conducted in the Langley VST to provide 6-DOF motion for flight dynamic analysis of the Orion LAV and CM. All tests used dynamically-scaled models. In general the average test conditions for each test were M = 0.04, V_∞ = 50 ft/sec, $\overline{q}_\infty$ = 3 psf, Re_d = 310,000. All models used in these tests were made using polycarbonate material fabricated from rapid prototyping techniques. The model's attitude and translational distance time histories are recorded accurately using non-obtrusive photogrammetric

techniques. From these time histories the motions of the models can be studied and used for aerodynamic parameter identification.

Test 45-AD was the first wind tunnel test of the LAV in the Orion CAP aerodynamic program. An early test to get a quick look at the stability of the LAV was desired because the Orion LAV had enough geometric and mass properties differences compared to the Apollo Launch Escape Vehicle (LEV) to cause uncertainty in the LAV's aerodynamics and flight dynamics predictions. Typically, the impetus for a dynamically-scaled VST test is to study dynamic stability. But this type of test also inherently captures the static aerodynamic effects. CFD had been used prior to Test 45-AD to produce static data. The CFD data showed that the LAV was neutrally to slightly statically unstable in nose-forward flight. The VST test validated this low level of static instability. Therefore, the value of this early test was not only to get an assessment of the dynamic stability but also confirmed the CFD results. Having confirmation of the static stability level was crucial since most GN&C simulation studies were using higher levels of static stability that were derived from the Apollo LEV. Additional benefits were that the test was executed quickly and at a low-cost, both in model fabrication and facility charges. Also, the quick turn around on useful data from the test was because the VST has been used for blunt body atmospheric free-flight studies for more than five decades. The parameters varied in this test were OML and mass properties. The OML configurations are closely matched to the final PA-1 configuration shown earlier; the main difference being different LAT lengths. At the time, the LAV was being designed to fly with canards for assisting reorientation, therefore, canards retracted and deployed were studied. The mass properties were varied because the LAV x_{cg} moves by approximately two feet during the first two seconds of flight due to abort motor propellant burn. Test 45-AD provided valuable early insight into the flight dynamics of the LAV for incompressible Mach numbers.

Test 48-CD was conducted by CAP in order to get additional information on the dynamically unstable CM. This additional data source was used in conjunction with the BR tests and FO tests in TDT to gain confidence in the dynamic aero characterization of the CM. Two dynamically-scaled 6.25% (*lRef* = 12.375 inches) CM models were built for this test. The flight cg of the CM has an offset in the z-direction for a lifting entry trajectory. This causes the model to fly across the tunnel test section limiting flight times. In order to study the dynamic motion for longer periods of time the z_{cg} offset was varied. Holding the x_{cg} at the full-scale flight value, all flights, regardless of the z_{cg} position, showed that the CM exhibits a divergent oscillatory motion. With the z_{cg} set to zero, the CM flew long enough that it eventually tumbled. A quick look of the effect of x_{cg} was conducted. These runs showed that, as with other blunt-body entry vehicles, as the x_{cg} is moved toward the heatshield the model becomes more dynamically stable. Also, this was the only test where an ablated heatshield shape was tested on a dynamically-scaled free-flight model. The ablated heatshield causes the CM to be asymmetric and, more potentially important to dynamic stability, changes the shoulder radius. The test results showed no change in the dynamic stability due to the ablation. Although unintended at test time, 48-CD provided models as well as valuable information for tests 82-CD, 108-CD, 109-CD, and 117-CD.

A cooperative free-flight test between the CAP and the CEV Parachute Assembly System (CPAS), Test 109-CD was conducted to characterize the dynamics of the CM while flying with the various IDAT drogue chute architectures. The test successfully characterized more than ten different drogue parachute configurations including single-point attachment, multi-point attachment, drogue out, reefed drogue (equivalent drag area of a full-scale reefed drogue), attachment location, and various riser line lengths. For each of the various configurations, flights were made with different initial conditions, such as displacement from trim attitude, pitch rate, yaw rate, and combinations of pitch and yaw rate to name a few. The test helped confirm that the program's choice of drogue configuration would provide satisfactory dynamics for the low-Mach flight regime. The test provided free-flight data that were used to compare against the 6-DOF simulation tool, Decelerator System Simulation (DSS). This is the main simulation tool used by the Entry GN&C group to ascertain the performance of the CM under the drogues and main parachutes. Comparing the test data to simulated 109-CD runs using DSS showed that the dynamic motion calculated by DSS was under-predicting the aerodynamic damping. This under-prediction result led to the forced oscillation test, 117-CD, intended to help in understanding why DSS was mis-modeling the damping. The analyses of these VST tests are ongoing and aimed at developing a physics based model that accounts for the contribution of the drogues to the damping of the CM motion.

IV. Crew Module Dynamic Stability

Sections IV and V will describe how the dynamic stability of the Orion spacecraft vehicles, CM, ALAS LAV, and PA-1 LAV was characterized with data from tests 18-CD and 27-AD. Recall these two tests were conducted in the NASA LaRC Transonic Dynamics Tunnel over a Mach range of 0.1 to 1.1 using the test medium of R134a. The data presented will be from the static force & moment, forced oscillation, and free-to-oscillate techniques. Keeping with the spirit of overview paper comparisons to other data sources will be through the references and only representative data sets from 18-CD and 27-AD will be provided.

A summary of the damping derivative characteristics is shown in figure 16 as a plot of damping derivative versus α for Mach numbers 0.2, 0.3, 0.45, 0.7, 0.8, 0.9, 0.95, and 1.1. Recall that the damping derivative represents the combined effect of angular rate and change in angle of attack. The data shows that the CM is dynamically unstable near $\alpha = 160°$ for $0.2 \le M \le 0.45$, transitioning to approximately neutrally stable over the entire alpha range for $M = 0.7$ to 0.8 then becoming unstable around $\alpha = 180°$ for $M \ge 0.9$. It should be noted that, based on the static data at the cg of $x_{cg}/D = 0.668$ and $z_{cg}/D = -0.030$, the CM will trim near 158° at $M = 1.1$ transitioning to trim near $\alpha = 174°$ for $M = 0.2$. Therefore, the unstable transonic points are outside of the trim range while the low-subsonic trim points are in the region of unstable damping.

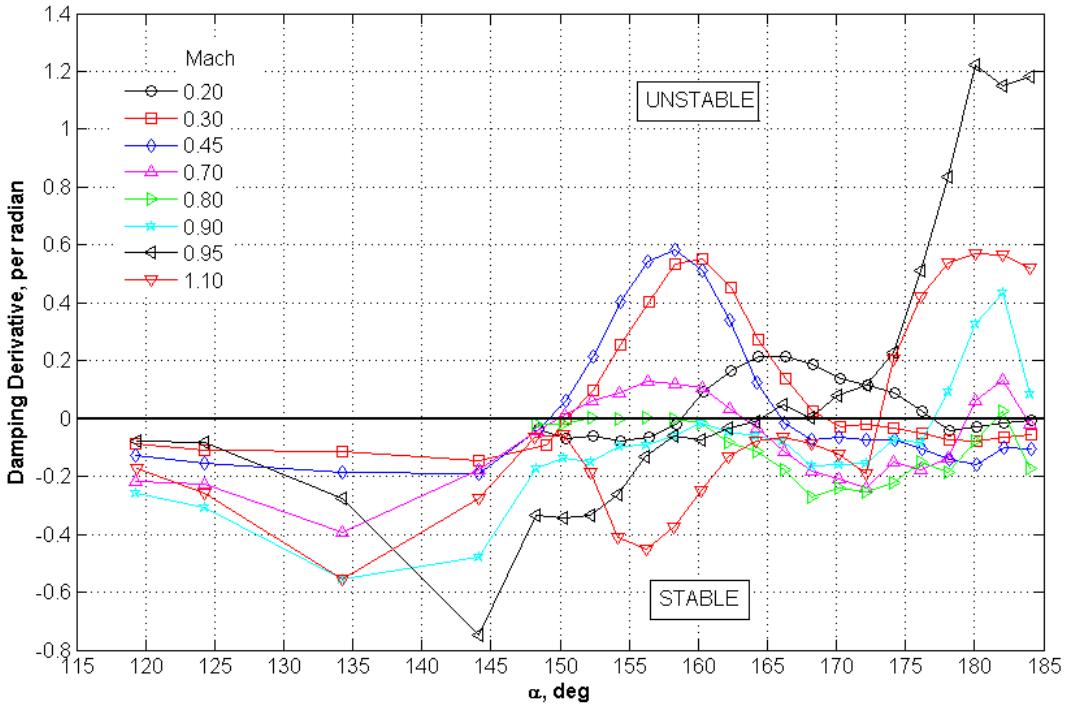

Figure 16. Effect of Mach number on the damping derivative for $x_{cg}/D = 0.668$, $z_{cg}/D = -0.030$, $Re_d = 5$ million.

A Reynolds number study was conducted during tests 8-CD (Ref. 13) and 18-CD (Ref. 14) to understand the sensitivity of pitch damping on this similitude requirement. Also, it would allow comparison to other CAP tests - namely, NASA LaRC 20-ft Vertical Spin Tunnel (VST) test described in Ref. 15 and NASA Ames Hypervelocity Free-Flight Aerodynamics Facility (HFFAF) ballistic range test described in Ref 12. The Reynolds number based on heatshield diameter, Re_d, for the VST and BR tests were on the order of 0.5 million. The Reynolds number study showed that above $Re_d = 5$ million, the damping derivative did not vary significantly with Reynolds number. Furthermore, at some Mach numbers there was not any difference in the damping derivative above $Re_d = 3$ million. Figure 17 demonstrates the Reynolds number effect on damping with a plot of damping derivative versus angle of

attack. Note that not only does the magnitude of damping change but the trend with α also changed significantly due to Reynolds number. During that study it was concluded that dynamic stability tests should be conducted nominally at Re_d = 5 million but not below 3 million. This conclusion concurs with Reynolds number studies conducted for static force and moment testing (Ref. 16). Furthermore, most of the Apollo program dynamic stability test data used in the construction of the Apollo aero database were from Re_d = 5 million data. Given the sensitivity of the damping derivative to Reynolds number, the use of the VST and BR data is limited to trends and deltas. While there are many advantages to using the VST and BR test techniques compared to the TDT, e.g., model and wind tunnel facility costs, such that the VST and BR were used productively in the Orion vehicles aerodynamic development, the aerodynamic database was developed from the TDT results.

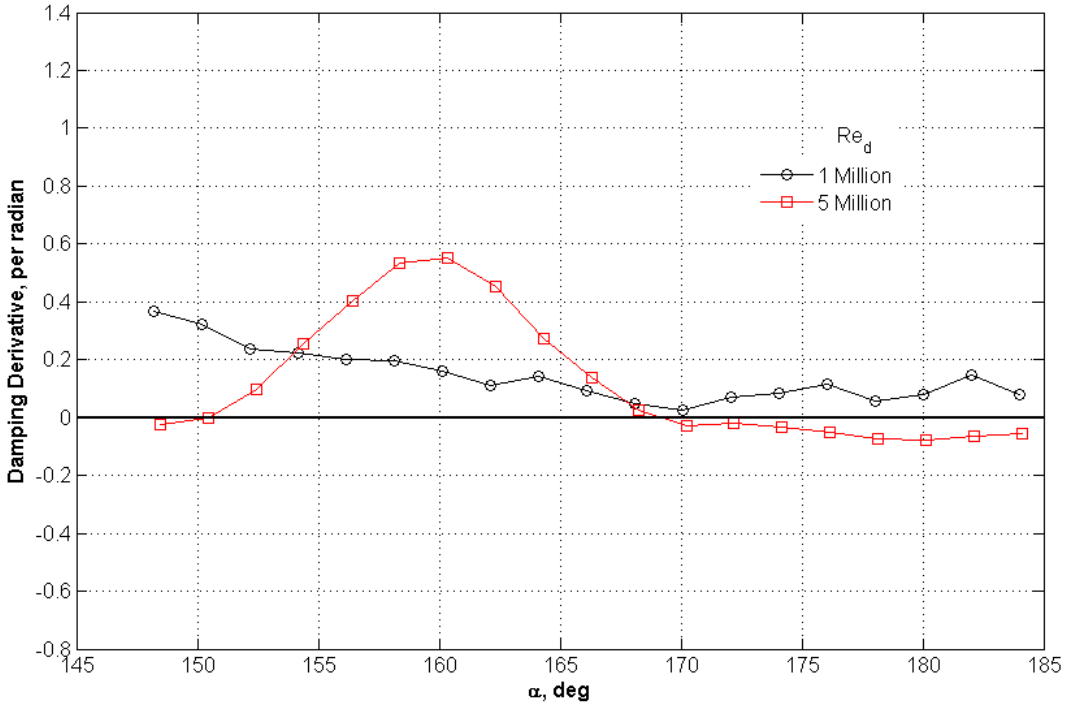

Figure 17. Effect of Reynolds number on CM damping derivative characteristics at M = 0.3, x_{cg}/D = 0.668, z_{cg}/D = -0.030, k = 0.137, $\hat{q}_{max}$ = 0.024.

The reduced frequency parameter, k, is one of the important similitude requirements when conducting forced oscillation testing. Matching k is required to capture the unsteady effects caused by oscillatory motion. The forced oscillation rig can change the frequency and amplitude of the motion independently. A simple increase in frequency without changing amplitude would also change the pitch rate. Therefore, in order to separate the effect of pitch rate from effect of frequency, the amplitude must be changed so that the angular rate at the mean α stays the same. Aerodynamic damping can be path dependent. In other words, the damping derivative can be dependent on the model's direction and the distance traveled during the motion. Reference 14 gives a detailed explanation of this but keeping within the scope of an overview paper only an example of the reduced frequency parameter is shown in Fig. 18 as a plot of damping derivative versus angle of attack. The largest effect of k occurs in the α range where damping is unstable. Also, the data shows that as k is increased the area of instability is reduced; however, this trend with k is not always the case, as will be shown in the section on LAV dynamic stability. The complete range of k that affects dynamic stability was not measured but the tests covered the range of k expected in flight.

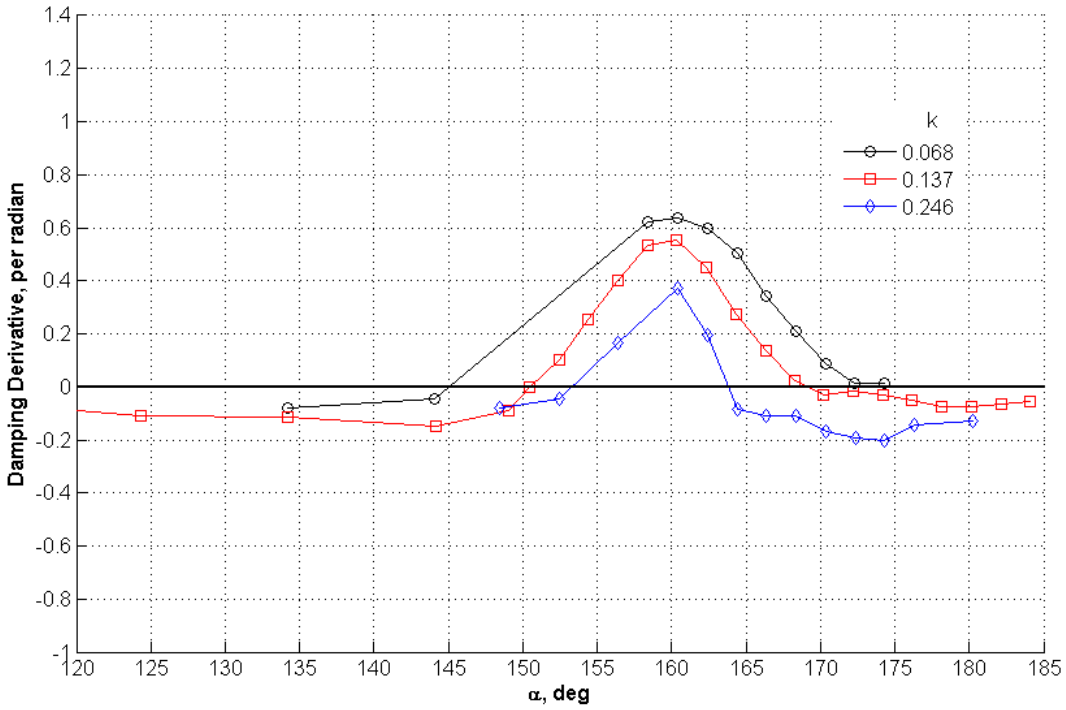

Figure 18. Effect of reduced frequency parameter, *k*, with a constant rate ($\hat{q}_{max}$= 0.024) on CM damping derivative. *M* = 0.3.

The non-dimensional angular rate is another important similitude requirement when conducting dynamic aero testing. Matching non-dimensional angular rate is required to assure that the induced flow field caused by the angular rate is accurately modeled. Since the desire is to separate the effects of rate from frequency (Strouhal number) the rate was varied by changing the amplitude while holding *k* constant. As mentioned in the last section this does not separate rate effects from path dependence. The effect of angular rate was measured over the Mach range of the test. At each Mach number the damping derivative was measured at four or more non-dimensional angular rates that cover the range expected in full-scale flight. An example of the angular rate effect on the damping characteristics is shown in Fig. 19 as a plot of damping derivative versus angle of attack. As with frequency effect, the largest rate effect on damping is in the unstable α region.

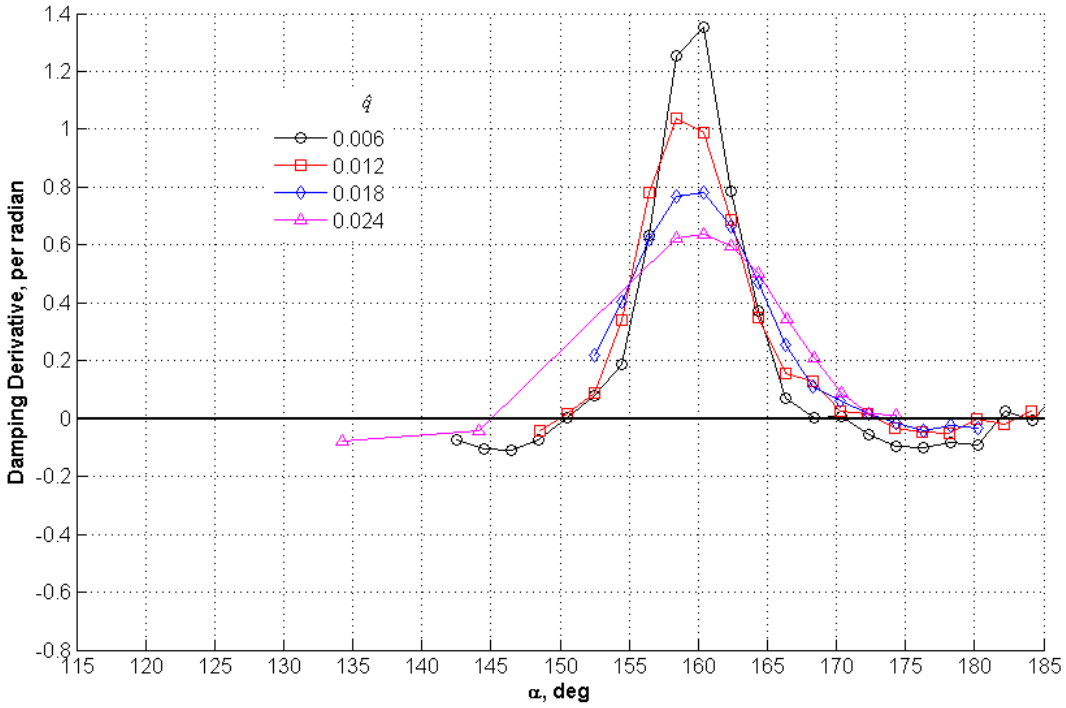

Figure 19. Effect of rate on CM damping derivative characteristics at M = 0.30, k = 0.068.

During test 27-AD the forced oscillation rig from test 18-CD was modified to allow free-to-oscillate (FTO) testing. The CM model was originally designed for the forced oscillation apparatus of test 8-CD. Therefore, the model was not designed to be dynamically-scaled for FTO testing. In 27-AD, the model was ballasted so that the cg of the model was on the axis of rotation but nothing was done to alter the moments of inertia. The inertia was measured and found to be approximately six times more than that dictated by similitude requirements. Figure 20 shows an example of a FTO α time history for M = 0.3. For the first 1.5s the model is held an α of 150° by a brake. At t = 1.5s the brakes are released resulting in the CM rotating under the influence of the static aerodynamic restoring force. Since the damping derivative is unstable in this α-range the oscillation amplitude grows with time until the model tumbles (t ~ 6s). A benefit of the FTO method is that it shows the integrated effects of the static and dynamic aerodynamics. Note that since the moment of inertia was heavier than it should have been for dynamic scaling requirements the frequency of the oscillations is lower than if scaling was correct. The result of the model tumbling is in concurrence with Apollo FTO tests and the Orion 48-CD tests which both showed that at this Mach number the CM will tumble if attitude hold via a control effector is not implemented. Also, the higher moment of inertia would not be expected to change whether or not the model motion diverges.

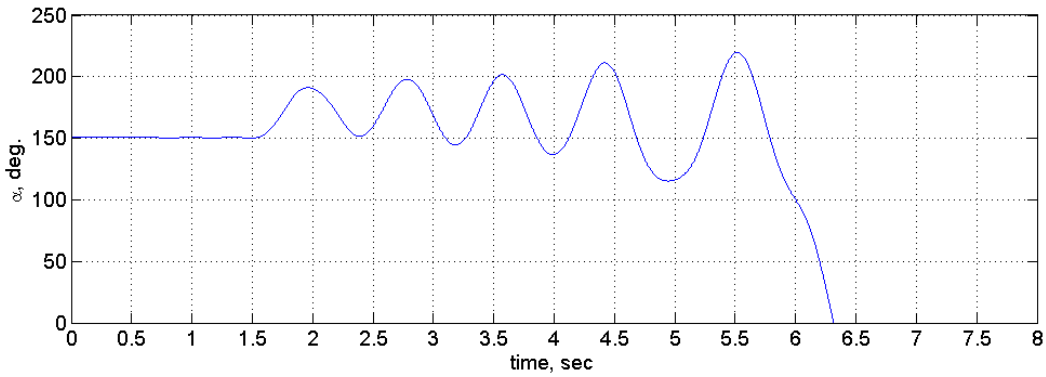

Figure 20. Free-to-oscillate angle of attack time history of the Crew Module at M = 0.3 starting with an initial α of 150°.

V. Launch Abort Vehicle Dynamic Stability

As in section IV for the Crew Module, this section gives a brief summary of the LAV dynamic stability for the ALAS and PA-1 configurations. The dynamic stability will be discussed in terms of the damping derivative as derived from the forced oscillation technique used in tests 18-CD and 27-AD. As described in the introduction section the LAV does a 180° maneuver in flight to orient the vehicle so that the CM can be released in a heatshield forward attitude required for successful landing. Therefore, the dynamic stability is investigated for $0 \leq \alpha \leq 360°$. This section shows the effect of configuration OML, Mach, angular rate, and reduced frequency parameter on the dynamic stability. It will use static force and moment and FTO data to assist in the explanation of the cause and effect of dynamic stability.

The Mach effect on the damping derivative for the ALAS LAV is shown in Fig. 21 with a plot of damping derivative versus α. The model is axis-symmetric about the x-body axis with the exception of the raceway and abort motor nozzles. Therefore, the damping derivative values should be almost symmetric about α = 180°. Other reasons, beyond the raceway and abort nozzles, for differences are repeatability and the fact that the α values between 0° to 180° were not exactly repeated from 180° to 360°. For all Mach numbers up to 1.1 the LAV is dynamically unstable heatshield forward (α ~ 180°). For all Mach numbers the model's dynamic stability increases as α increases from 0° to ~ 50°. This trend in damping coincides with the linear normal force coefficient shown in this same α-region (see Fig. 22). Above this α and until α ~140° the damping derivative has a very non-linear trend with α. Additionally, the model becomes dynamically unstable for a portion of that α range with the exception of M = 1.1. Again referring to the static aerodynamics of Fig. 22, this nonlinear trend in the damping derivatives and subsequent instability is directly associated with the non-linear static aerodynamics. The non-linear static aerodynamics indicates an abrupt flow topology change. The α where the static aerodynamics changes abruptly occurs at the same α where the dynamic aero changes abruptly. The static data for Fig. 22 are only for M = 0.3 but data at the other Mach numbers show similar characteristics, with Mach number affecting the α where the normal force coefficient breaks and how abruptly it breaks. This change in flow topology is what determines the α where the peak instability occurs. Figure 21 shows that starting around α = 135° for $M \leq 0.9$ and α = 150° for M = 1.1 the model becomes less stable dynamically, reaching the peak instability at α = 180°. The α-range of unstable values of the damping derivatives almost exactly corresponds to the linear, strongly stable portion of the static pitching moment curve shown in Fig. 22. In this same α-range, the axial and normal force coefficients are nearly constant indicating that the flow is probably separating near the shoulder of the heatshield. The dynamic instability in the α-range, 150° to 210°, is probably due to the asymmetric flow separation around the blunt body formed by the heatshield.

The preceding discussion of the ALAS configuration dynamic stability is similar for the PA-1. Rather than repeat the same discussion, configuration effects on dynamic stability will be discussed by comparing the ALAS damping derivatives in Fig. 21 to the PA-1 damping derivatives shown in Fig. 23. In this comparison only the M = 0.7 and

below data of the ALAS configuration from Fig. 21 will be used since this coincides with the same range for PA-1 in Fig. 23. Also, note that although the current flight cg of the ALAS is further aft than the PA-1, while at the time the 27-AD test was conducted they were the same. The first comparison is in the range of damping values between the two configurations. The PA-1 configuration has a magnitude range of -6 to 6 compared to -8 to 8 for the ALAS configuration which is a significant increase in range. As the length of the vehicle, axis of rotation, reference dimensions and heatshield are the same for both configurations it is concluded that this magnitude change is caused by the significant change in OML between the heatshield shoulder and the abort motor nozzles. As described for the ALAS configuration in the preceding paragraph the PA-1 also shows three α-ranges where the damping derivative shows a change in character. For the sake of comparison these ranges will be approximated as: Range 1: $0° < \alpha < 40°$; Range 2: $40° < \alpha < 135°$; Range 3: $135° < \alpha < 180°$. The trend in Range 1 is very similar for both configurations. The non-linear region of range 2 has much less variation for the PA-1 than the ALAS configuration. In range 3 the interesting difference is the inflection in the curve near $\alpha = 150°$ for the PA-1 configuration that is not observed in the data for the ALAS. Although there is no direct evidence from the measured data, the source of this inflection is probably due to the difference in the OML at the shoulder of the heatshield. The PA-1 configuration has a sharp edge near the shoulder whereas the ALAS is rounded in the same region.

Returning to the discussion of the ALAS, Fig. 24 is a plot of the FTO α time history at $M = 0.4$ with the model released from an initial condition of zero angular rate and $\alpha = 175°$ which is near trim as shown with the static data in Fig. 22. Unlike the CM model the LAV configurations were dynamically-scaled. Therefore, the motion observed in Fig. 24 can be scaled to full-scale flight. Since this is an 11% -scale model the rates will be approximately three times faster in the wind-tunnel test than in flight. Using the static data of Fig. 22, which shows a strong restoring moment in this α-range and the dynamic aero data of Fig. 21 which shows dynamic instability in this α-range, the plot shows that it has a divergent oscillation about its static trim point of approximately $\alpha = 178°$ until it flips to a high α stable trim point near $\alpha = 90°$. It has many overshoots at this $\alpha = 90°$ trim point because, as Fig. 21 shows, the damping derivative is slightly positive around this α. The cg at which this test was conducted represents a location near the beginning of abort initiation. The ALAS suffers from low static stability during tower forward flight, and a means for a more forward cg have been studied. While this might solve the tower-forward static stability issue it worsens the heatshield-forward flight stability by decreasing static stability and increasing the probability of reaching an $\alpha = 90°$ stable trim point due to divergent oscillations.

As with the CM forced oscillation tests, the LAV tests were designed to cover the non-dimensional angular rate and reduced frequency parameter expected in flight. Since the LAV configurations had never flown when this test was conducted, only 6-DOF simulations and the FTO data of this test could be used to determine the requisite range of these two similitude requirements. The need to test at the correct k and angular rates for a configuration that has never flown underscores the advantage of having a FTO technique that can be used in the same test with zero down time required to switch between other techniques. The effect of angular rate on the ALAS damping derivative is shown in Fig. 25 as a plot of the damping derivative versus α for three angular rates. The data shows a significant sensitivity to angular rate with the maximum sensitivity near $\alpha = 180°$. The sensitivity to rate is only in the region of instability. Also, it shows that as rate is increased the model becomes more dynamically stable. Even so, the model is never completely dynamically stable in heatshield-forward attitudes over the range of non-dimensional angular rates used in the test. The effect of the reduced frequency parameter on dynamic stability is shown in figure 53 as a plot of damping derivative versus α for $M = 0.4$. As with angular rate the damping derivative is most sensitive to frequency near the dynamically unstable α region near 180°. At $M = 0.4$ the data shows that as frequency is increased the model becomes significantly more unstable. At this Mach number the frequency sensitivity diminishes for stable damping derivative values. So as to show that these trends are not seen at all Mach numbers the damping derivative as a function of α for $M = 0.7$ for three values of k is shown in Fig. 27. At this Mach number the trend with k is non-linear and the sensitivity persists into the stable damping derivative range. The onset of significant compressibility effects is probably the cause of the change in character from $M = 0.4$. This effect with Mach underscores the need to match Mach scaling as well as Froude scaling laws as much as possible.

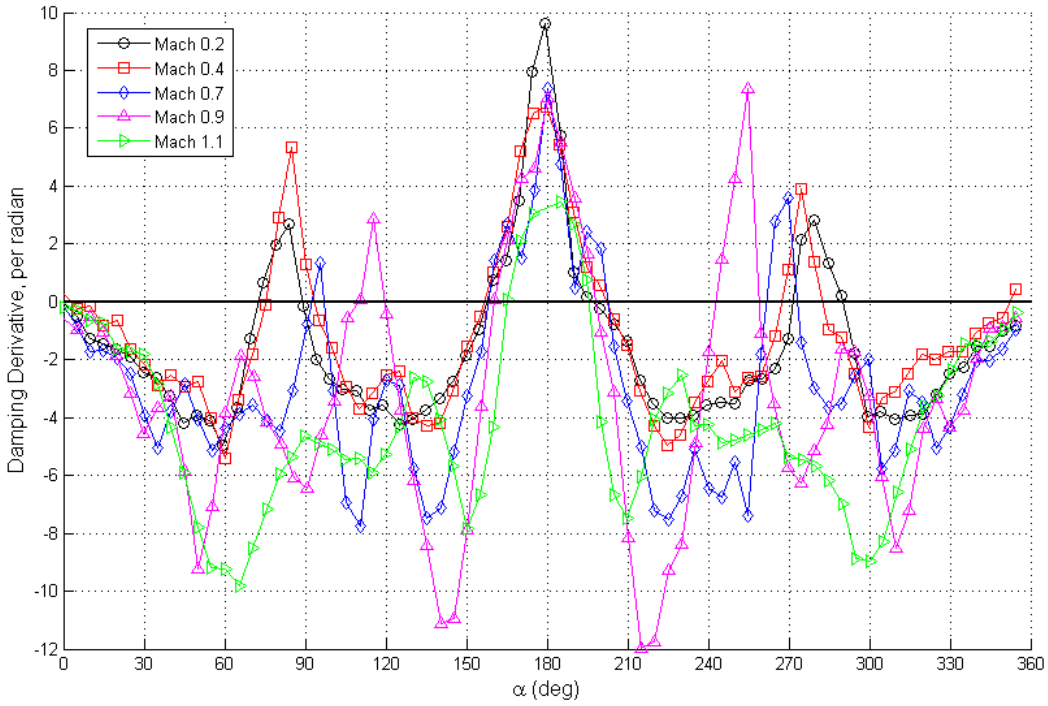

Figure 21. Effect of Mach number on the damping derivative for the ALAS LAV. Re_d = 5 million

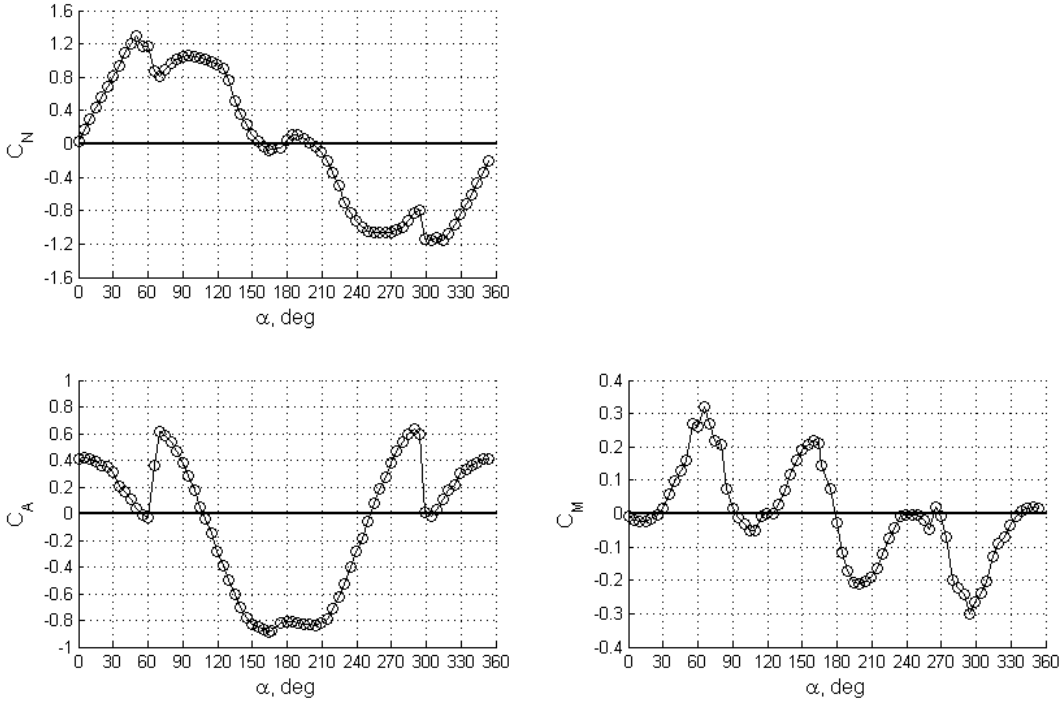

Figure 22. Static force and moment data for the ALAS LAV at *M* = 0.4. Re_d = 5 million

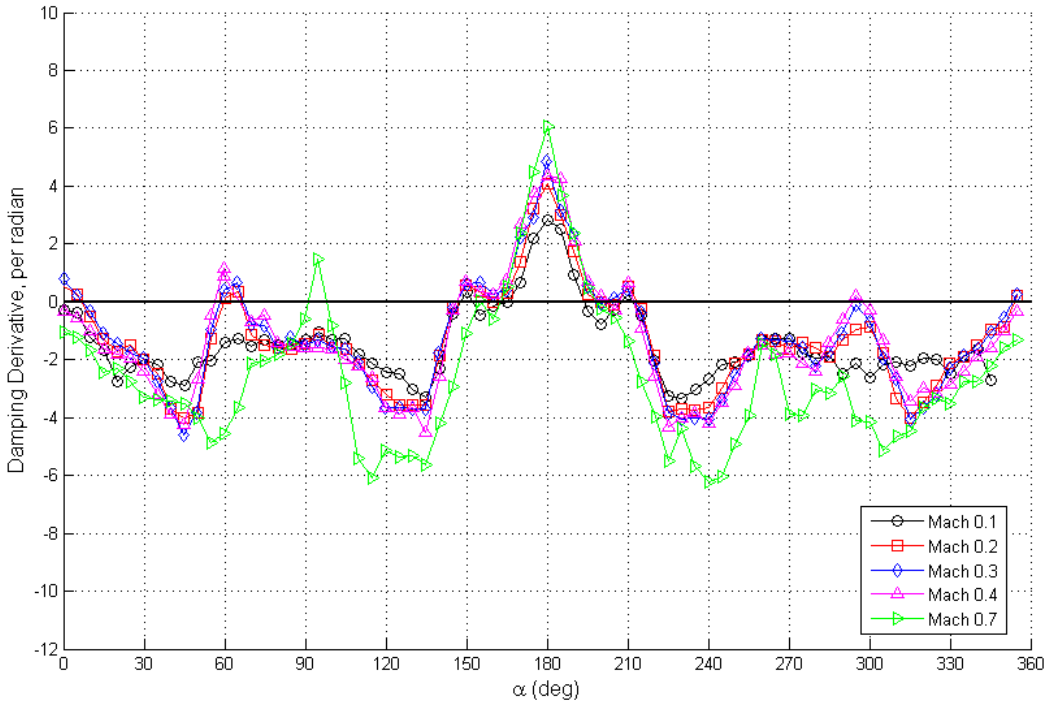

Figure 23. Effect of Mach number on the damping derivative for the PA-1 LAV. Re_d = 5 million

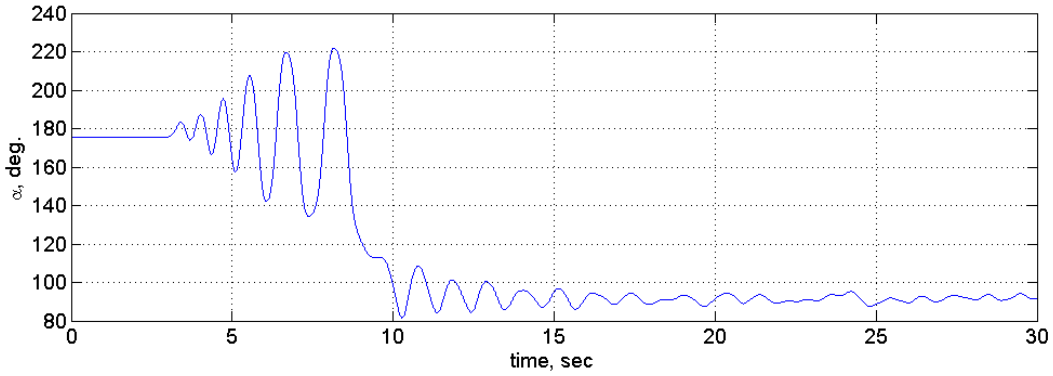

Figure 24. Free-to-oscillate α time history for the ALAS configuration at M = 0.4 starting with an initial α at 175°.

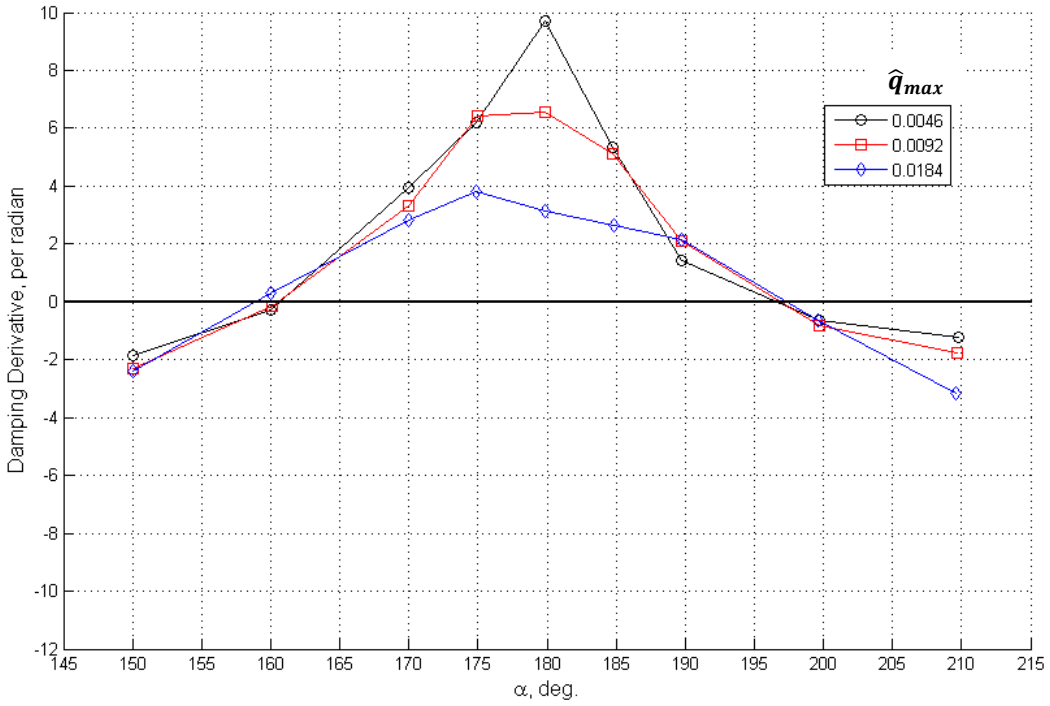

Figure 25. Effect of non-dimensional angular rate on the damping derivative of the ALAS configuration, i = 0.4.

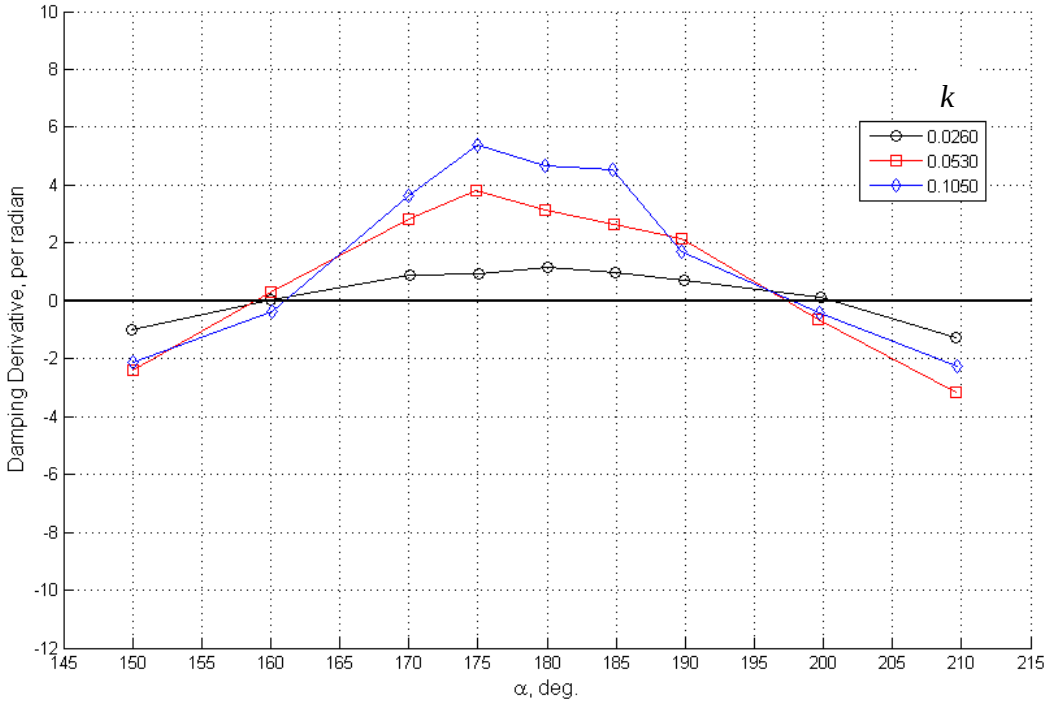

Figure 26. Effect of reduced frequency parameter at M = 0.4 for the ALAS configuration. $\hat{q}_{max} = 0.184$.

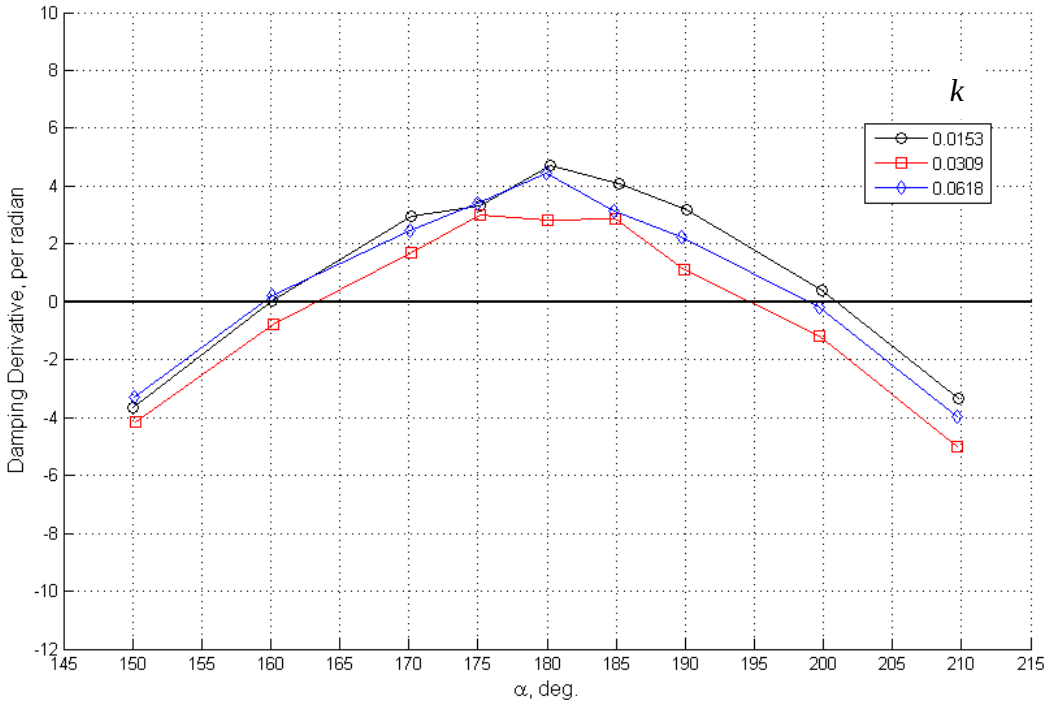

Figure 27. Effect of reduced frequency parameter at M = 0.7 for the ALAS configuration. $\hat{q}_{max}$ = 0.108.

VI. Summary

In order to design the next manned spacecraft NASA invested in an aerodynamic program that invoked multiple dynamic test techniques to characterize the dynamic stability of the Orion vehicles. The importance of accurate characterization of the dynamic stability was historically known from programs like Apollo and many of the Mars entry vehicle programs. The Orion program used the following dynamic test techniques: free-flight outdoor and indoor ballistic ranges and Vertical Spin Tunnel, forced oscillation, and free-to-oscillate. Using the full suite of dynamic test techniques provided detailed insight into the aerodynamic damping characteristics of the Orion vehicles. Although many of the test techniques have been in use since the Apollo program, the Orion program invested in the development of a new forced oscillation technique for the LaRC Transonic Dynamics Tunnel for aerodynamic database development. Dynamic stability plays a critical role in the entry flight dynamics of the CM especially when it is in free-flight (closed-loop control system inactive). This flight regime occurs in the M < 0.7 range where dynamic stability plays a larger role in the overall aerodynamics. Dynamic stability affects the flight dynamics of the LAV during its high rate reorientation from nose-forward to heatshield forward phase and the subsequent overshoots about the trimmed heatshield forward attitude. The results of the tests showed that both the CM and LAV are dynamically unstable in heatshield forward flight. Furthermore, the tests measured the sensitivity of the damping derivative to Mach, α, Re_d, reduced frequency parameter, non-dimensional pitch rate, and geometry. The Reynolds number studies found that a nominal Re_d = 5 million was required to accurately measure the damping derivatives. It was also found that the sensitivity to the similitude parameters were the greatest in the α-ranges of unstable damping. The qualitative assessment of the free-flight tests agrees with the captive test techniques that both the CM and LAV are dynamically unstable in heatshield forward flight. While the damping derivatives calculated from the ballistic range tests agree with the forced oscillation test results in general, there were areas of significant discrepancy that warrant further research. The majority of the dynamic stability tests are complete for the Orion program and the data has been integrated into the 6-DOF simulation tools used by various GN&C groups. Currently,

research and development continues in the area of improving the damping model of the CM plus drogue system by using dynamic test techniques in the NASA LaRC Vertical Spin Tunnel.

Acknowledgments

The Orion CAP program dynamic aero tests were conducted by several engineers at different NASA centers – Jeff Brown, Gary Chapman, Mike Fremaux, Sue Grafton, Mark Schoenenberger, Debi Tomek, Mike Wilder, and Leslie Yates. The authors would like to acknowledge their contribution to obtaining a detail characterization of the dynamic stability of the Orion Crew Module and Launch Abort Vehicle. Also, the authors would like to acknowledge the many helpful discussions with some of the Apollo Program engineers who characterized the dynamic stability for the Apollo vehicles – Bass Redd, Joe Gamble, Rick Barton, and Paul Romere.

References

[1]Igoe, W. B., and Hilje, E. R., "Transonic Dynamic Stability Characteristics of Several Models of Project Mercury Capsule Configurations," NASA-TM X-554, 1961.

[2]Moseley, W. C., Jr. and Martino, J. C., "Apollo Wind Tunnel Testing Program – Historical Development of General Configurations," NASA TN D-3748, 1966.

[3]Wolowicz, C. H., and Bowman, J. S., "Similitude Requirements and Scaling Relationships as Applied to Model Testing," NASA TP-1435, 1979.

[4]Gainer, T. G., and Hoffman, S., "Summary of Transformation Equations and Equations of Motion Used in Free-Flight and Wind-Tunnel Data Reduction and Analysis," NASA SP-3070, 1972.

[5]Ross, J. C., "Aerodynamic Testing in Support of Orion Spacecraft Development," AIAA Paper 2007-1004, 2007.

[6]Klein, V. and Morelli, E. A., "Aircraft System Identification: Theory and Practice," AIAA Education Series, AIAA, Virginia, 2006.

[7]Tomek, D., "The Next Generation of High-Speed Dynamic Stability Wind Tunnel Testing," AIAA-2006-3148, 25th AIAA Aerodynamic Measurement Technology and Ground Testing Conference, June 2006.

[8]Owens, D. B., Brandon, J. M., Croom, M. A., Fremaux, C. M., Heim, E. H., and Vicroy, D. D., " Overview of Dynamic Test Techniques for Flight Dynamics Research at NASA LaRC," AIAA Paper 2006-3146, 2006.

[9]Aubuchon, V.V., Owens, D.B., and Fremaux, C.M., "Drogue Parachute Effects on the Orion Crew Module Aerodynamics," 29th Applied Aerodynamics Conference, AIAA, Honolulu, HI, 27-30 June 2011 (submitted for publication).

[10]Redd, B., Olsen, D. M., Barton, R. L., "Relationship Between the Aerodynamic Damping Derivatives Measured as a Function of Instantaneous Angular Displacement and the Aerodynamic Damping Derivatives Measured as a Function of Oscillation Amplitude," NASA TN D-2855, June 1965.

[11]Yates, L. A. and Chapman, G. T., "Analysis of Data from Ballistic Range Tests for an Untrimmed CEV Model," Task RAA002, NASA-LaRC December 2006.

[12]Brown, J. D., Bogdanoff, D. W., Yates, L. A., and Chapman, G. T., "Static and Dynamic Aero Coefficients for Lifting CEV Capsules in Free Flight Between Mach 0.7 and Mach 1.25," AIAA Paper 2008-1232, 2008.

[13]Tomek, D. and Owens, D. Bruce; "CEV Dynamic Damping Test in the Transonic Dynamics Tunnel," EG-CEV-06-23, NASA Langley Research Center, January 2007.

[14]Owens, D. Bruce and Tomek, D.; "18-CD Subsonic-Transonic Crew Module Dynamic Stability Test in the NASA LaRC Transonic Dynamics Tunnel," EG-CEV-06-23, NASA Langley Research Center, February 2009.

[15]Fremaux, C. M.; "Low Subsonic Dynamic Stability Test of the Orion Crew Module in the NASA LaRC 20-Foot Vertical Spin Tunnel," EG-CAP-08-122, NASA Langley Research Center, June 2008.

[16]Bell, J.H., "Test 5-CA Final Report," CEV Aerosciences Project, Rept. EG-CEV-06-19, NASA Ames Research Center, March 2006.